

# 3D model based stereo reconstruction using coupled Markov random fields

Evelyne Lutton

► **To cite this version:**

Evelyne Lutton. 3D model based stereo reconstruction using coupled Markov random fields. [Research Report] RR-1951, INRIA. 1993. <inria-00074722>

**HAL Id: inria-00074722**

**<https://hal.inria.fr/inria-00074722>**

Submitted on 24 May 2006

**HAL** is a multi-disciplinary open access archive for the deposit and dissemination of scientific research documents, whether they are published or not. The documents may come from teaching and research institutions in France or abroad, or from public or private research centers.

L'archive ouverte pluridisciplinaire **HAL**, est destinée au dépôt et à la diffusion de documents scientifiques de niveau recherche, publiés ou non, émanant des établissements d'enseignement et de recherche français ou étrangers, des laboratoires publics ou privés.



INSTITUT NATIONAL DE RECHERCHE EN INFORMATIQUE ET EN AUTOMATIQUE

*3D Model Based Stereo  
Reconstruction using Coupled  
Markov Random Fields*

Evelyne LUTTON

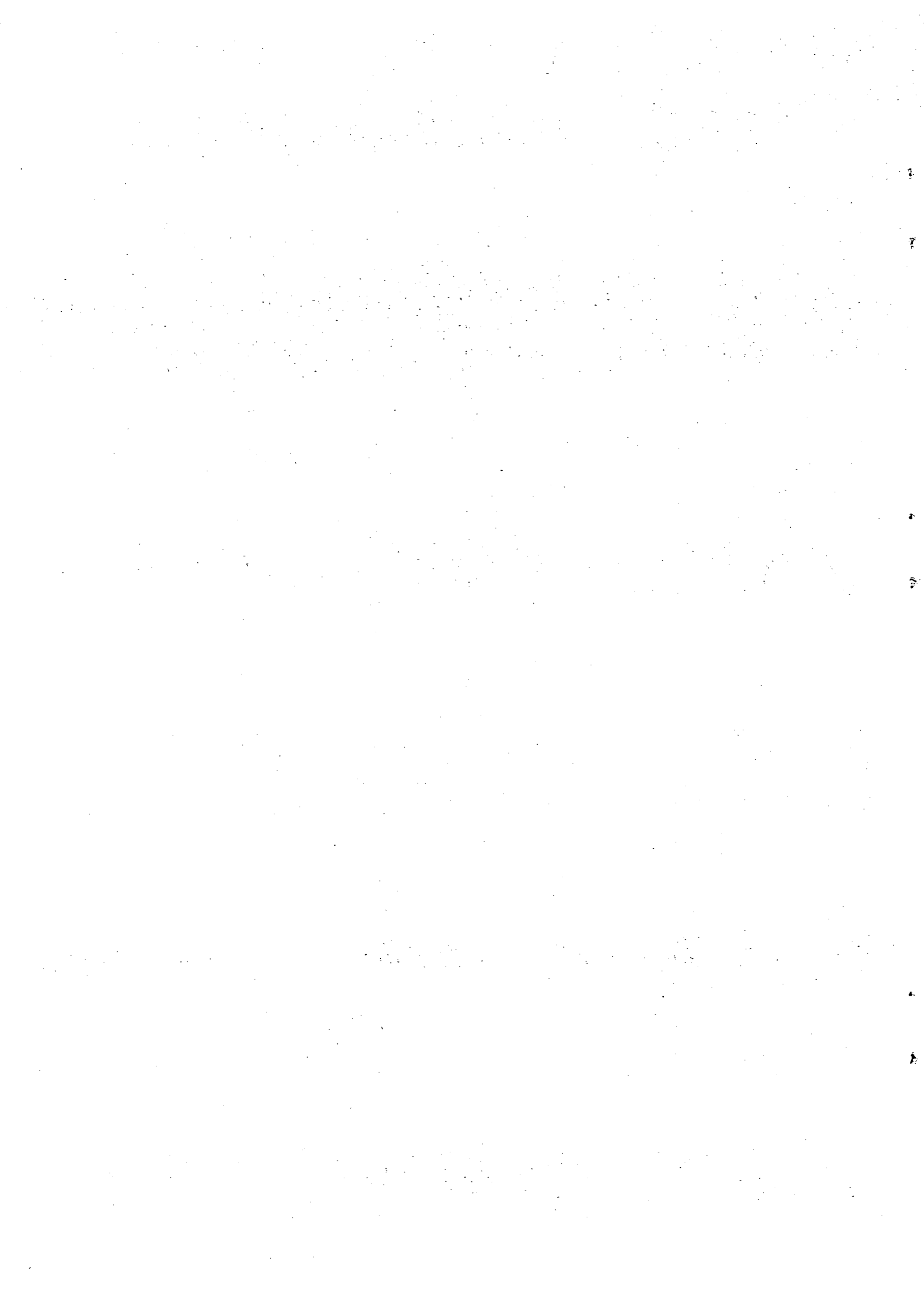
N° 1951  
Juin 1993

PROGRAMME 4

Robotique, image  
et  
vision

*R*apport  
*de recherche*

1993



# 3D Model Based Stereo Reconstruction using Coupled Markov Random Fields

## Stéréo-reconstruction fondée sur un modèle, à l'aide de Champs Markoviens Couplés

*Evelyne LUTTON*

INRIA - Rocquencourt

B.P. 105, 78153 LE CHESNAY Cedex, France

Tel : 33 1 39 63 55 23

Fax : 33 1 39 63 53 30

Evelyne.Lutton@inria.fr

### Abstract

*A lot of methods have been proposed in the field of stereo-reconstruction. We address here the problem of model-based tridimensional reconstruction from an already segmented and matched stereo pair. This work is a continuation of the work presented in [13] and [14], concerning the reconstruction problem. We study here a method based on Markov random fields, which allows the a priori segmentation and matching to be refined during the reconstruction of the 3D surfaces. A new segmentation and matching is then produced which respects the 3D coherence (or equivalently the disparity coherence) of each segmented region-pair. In this first approach, we use simple segmentation energies for each image (without line processes), plus a coupling term between the left and right images, associating planes (as surface primitives) with each region pair. This is the justification for using coupled Markov random fields. We present results on synthetic and real images. These preliminary results allow us to assess the feasibility of a hierarchical stereo reconstruction method with no a priori segmentation and matching.*

### Keywords :

Image analysis, computer vision, 3D stereo-reconstruction, model-based stereo, markov random fields.

### Résumé

*Notre problème est ici d'étudier la reconstruction tridimensionnelle fondée sur un modèle à partir d'une paire stéréo déjà segmentée et mise en correspondance. Ce travail fait suite à une méthode présentée dans [13] et [14], à propos du problème de reconstruction stéréo. Nous étudions ici une méthode fondée sur des champs Markoviens, ce qui nous permet de remettre en question la segmentation et le matching a priori, au cours du processus de reconstruction des surfaces 3D. Une nouvelle segmentation et une nouvelle mise en correspondance sont ainsi produites, respectant la cohérence 3D (ou de façon équivalente la cohérence des disparités) de chaque paire de région segmentée. Dans cette première approche, nous employons des énergies de segmentation simples pour chaque image (sans processus de ligne) plus un terme de couplage entre les images gauche et droite, en associant des plans (comme primitives de surfaces) à chaque paire de régions. C'est de là que vient la notion de couplage de deux champs de Markov. Nous présentons des résultats sur des images de synthèse, puis sur des images réelles. Ces résultats préliminaires nous permettent de conclure sur la faisabilité d'une méthode hiérarchique de reconstruction stéréo sans l'aide d'une segmentation et d'une mise en correspondance a priori.*

# 1 INTRODUCTION

In the field of stereo reconstruction, the model-based approach has been largely recognized as useful to obtain dense disparity maps, or reconstructed surfaces. Our purpose is to reconstruct tridimensional surfaces (in a first approach, planar facets) from a segmented and matched stereo pair. Our preceding work on this topic ([22], [13], [14]), leads us to the conclusion that reconsideration of the a priori segmentation and matching is necessary in order to improve the 3D reconstruction results.

Supposing that we have already segmented and matched a stereo pair, we search for a plane associated with each pair of matched regions (see figure 1). The information about the reconstructed facets permits us to reconsider the initial classification of image pixels. The new segmentations then produced suggest new 3D facets, and so on. It could thus be considered as an iterative process, i.e. more simply as a pair of parameterized coupled Markov Random Fields, as we will see later.

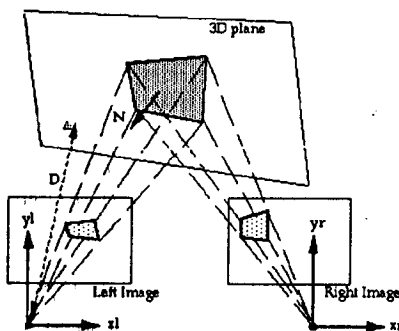


Figure 1: Planar facet reconstruction

The isolated problem of stereo reconstruction using surface models was already studied, mostly in the case of plane models. The approaches used are of two types :

- using a disparity map (on zero crossings, or contours, for example), and fitting surface models to it, see for example [24],
- directly using surface models to compute dense disparity maps ; see [17, 22, 19].

In the first approach, surface models other than planar facets have been used, while in the second approach the methods were developed only in the case of planar surfaces. In this latter approach, indeed, an explicit transformation between the left and right images is needed. This transformation is used either in a matching criterion (as in [17]) or directly in a reconstruction criterion to be minimized, as in [22], where it is approximated, or as in [19], where it is used in an energy function in a Markov Random Field.

The use of Markov Random Field (MRF) in stereovision is not new, and recently several important methods have been advanced to hypothesize dense disparity maps, and use surface models, or disparity uniformity criteria. We can distinguish here also two main methods : reconstruction of one disparity map considered itself as a MRF (for example [3, 5]), or more rarely, the use of a coupled MRF, one for each image of the stereo pair [19, 4] ; in this case, the dense disparity map is implicitly obtained with the reconstructed surface patches.

We preferred the second approach, which is to couple two MRFs, because :

- the notion of neighborhood is not so obvious for a disparity map ; sometimes, the reconstructed 3D points corresponding to those of the disparity map can be very sparse, even in continuous areas ; we prefer to maintain the classical image segmentation neighborhood system,
- we can take into account non-matched regions or occlusion areas in the two images, which is not possible with a disparity map,

- it relates more naturally to the image segmentation schemes ; indeed we can segment areas of one of the two images, which are not matched or reconstructed.

In this paper, we present a method to hypothesize planar facets, starting from an initial segmentation and matching (as in figure 2). We currently use a region growing segmentation and a matching technique proposed in [23, 18]. We suppose that we know the calibration of the two cameras, i.e. the relative rotation and translation, and the internal parameters (focal length, center of projection) of each camera. Our problem is thus : knowing the two projections (i.e. a pair of matched regions) of an unknown 3D facet, search its 3D supporting plane, and improve the segmentation and matching according to the criterion of 3D coherence.

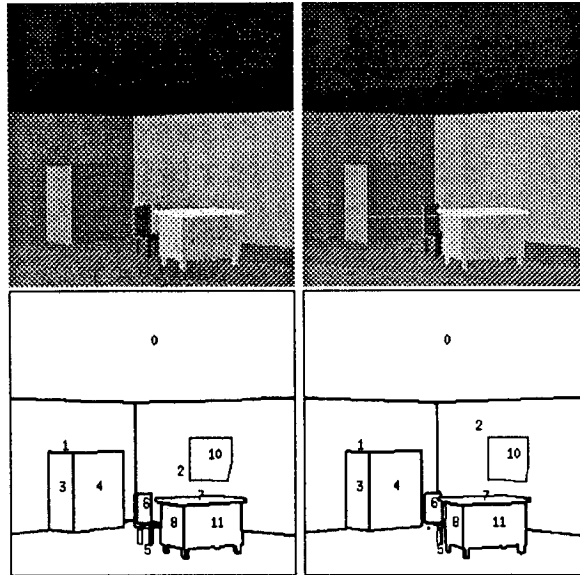


Figure 2: Original 256\*256 synthesized color stereo pair (red channel) and matched pair

## 2 COUPLED MARKOV RANDOM FIELDS

In a lot of early vision applications, Markov Random Field have provided an interesting theoretical frame, furnishing very efficient methods for a large variety of applications. The common hypothesis of these approaches is that we consider the observations as sufficiently noisy or incomplete that it is not possible, based on them alone, to determine the solution in a unique way (ill-posed problem). Given a probabilistic model for the observations, prior knowledge about the solution is encoded by supposing that some functions (for example the smooth ones) are more likely to occur than others, within the space of all possible ones.

We will here briefly describe the MRF approach ; a more extensive discussion is given, for example, in [7] or in [15].

### 2.1 Markov Random Field approach

Let  $Lab = \{Lab_s\}$  be an image, defined on a finite lattice of sites (or pixels) :  $\Omega = \{s = (i, j); i \leq i, j \leq M\}$ . Let  $N(s)$  be the neighborhood of site  $s$ . The image is considered as a Markov Random Field relative to the neighborhood set  $\{N(s)\}_{s \in \Omega}$  if it verifies :

$$P(Lab_s | Lab_r, r \in \Omega - \{s\}) = P(Lab_s | Lab_r, r \in N(s) - \{s\})$$

It means that the conditional distribution of the value of a pixel  $s$  depends only on the values of its neighborhood pixels.

Another important characteristic comes from the Hammersley-Clifford theorem, which gives the equivalence of such a random field with a Gibbs distribution :

$$P_T(Lab) = \frac{\exp - \frac{U(Lab)}{T}}{Z_T}$$

where  $U(Lab)$  is an energy function :  $U(Lab) = \sum_{t \in C} V_t(Lab)$ . Here,  $C$  is the set of cliques corresponding to the neighborhood set  $N(s)$  (see figure 3), and  $V_t(Lab)$  is a potential function expressing the local constraints on the image (for example smoothness constraints).  $V_t(Lab)$  depends only on the values  $Lab_s, s \in \Omega$ .  $T$  and  $Z_T$  are constants :  $T$  is the temperature, and  $Z_T$  is a normalization constant, called the partition function ( $P_T(Lab)$  is a probability).

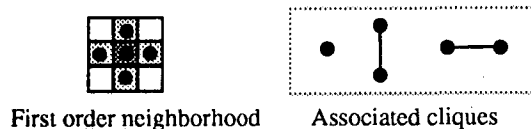


Figure 3: First order neighborhood system

## 2.2 MAP estimation

Using Bayes' rule, the conditional probability of obtaining an image  $Lab$  from a given set of data  $I$ ,  $P(Lab|I)$ , may be written :

$$P(Lab|I) = \frac{P(I|Lab)P(Lab)}{P(I)}$$

where  $P(I|Lab)$  is the data term and  $P(Lab)$  is the prior probability. Since  $P(I)$  is fixed :

$$P(Lab|I) \propto P(I|Lab)P(Lab)$$

The most common method to estimate  $I$  is to maximize the a posteriori probability, i.e. to minimize the corresponding energy function :

$$U(I|Lab) + U(Lab).$$

$U(Lab)$  is the preceding a priori energy of an image, and  $U(I|Lab)$  enforces coherence with the data. A simple (but slow) method to do the minimization is simulated annealing, which decreases the temperature  $T$  while using for example the Gibbs sampler ; for more details see [7].

## 2.3 Coupling MRF

The notion of coupled MRF has appeared in such applications as data fusion [1] and motion analysis [9]. The common idea of these applications is that several interacting MRFs are simultaneously minimized. This approach is not theoretically different from the general one, as defined before. Indeed, coupled MRFs are equivalent to a unique one, but with extra variables and modified neighborhoods.

In our application, we have constructed two classical segmentation MRFs, one for each image, plus an interaction between matched pixels. This system is equivalent to a MRF on the union of the two images, with an extended neighborhood, allowing interactions between the two images, see figure 4.

Notice that we have also to consider some special border effects where the neighborhood is not complete, that is :

- when the pixels have no extended correspondent : complete first order neighborhood, but with no correspondent on the other image (we will see that it is the case of non-matched pixels in a stereo pair),

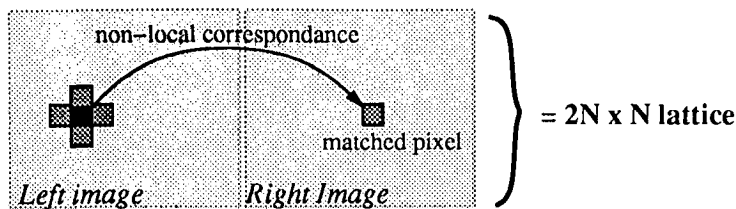


Figure 4: Extended neighborhood : for our application, the nonlocal correspondance is the parameterized pixels transformation described in the figure 5

- at the limits of the two images (incomplete first order neighborhood, with or without correspondent on the other image).

We thus minimize an energy function wich can be decomposed into three terms :

$$U(Lab_{Left}, Lab_{Right} | I_{Left}, I_{Right}) = U_{Seg}(Lab_{Left} | I_{Left}) + U_{Seg}(Lab_{Right} | I_{Right}) + U_{Coupl}(Lab_{Left}, Lab_{Right} | I_{Left}, I_{Right})$$

In the next sections, we will describe these terms in detail.

### 3 ENERGY EXPRESSIONS

#### 3.1 Image energies : $U_{Seg}$

For simplicity, we choose the simplest form of segmentation energy, which is based on the first order neighborhood (see figure 3). Of course we could use line processes which are sometimes very efficient (see [6]), but we preferred in a first approach to have the least possible number of terms and variables. Indeed, the choice (or estimation) of the relative weights of the different terms is itself a difficult problem.

$U_{Seg}$  is thus a combination of two terms : coherence to the data and smoothness constraint.

$$U_{Seg}(Lab | I) = \frac{1}{2\sigma_{Lab}^2} \sum_{s \in \Omega} (I_s - \mu_{Lab_s})^2 + \sum_{\{s,t\} \in C(\Omega)} \zeta[Lab_s - Lab_t]$$

$Lab$  is the associated image of labels,  $\mu_{Lab_s}$  is the mean of the region of the image having  $Lab_s$  as label.  $\sigma_{Lab}$  is the variance tolerated on uniform regions, it is a constant on the whole image.  $C(\Omega)$  is the set of first order cliques on the image  $I$  (4-neighborhood) ; see figure 3.  $\zeta$  represents the function :

$$\zeta(x) = \begin{cases} 0 & \text{if } x = 0 \\ 1 & \text{else} \end{cases}$$

The  $\sigma_{Lab}$  parameter is used also to measure the relative importance of the smoothness terms.

For color images, the coherence to the data term is the mean value of the terms corresponding to each channel ; the smoothness term remains the same.

#### 3.2 Coupling energy : $U_{Coupl}$

The coupling energy is based on a parameterized transformation between left and right images, so this energy measures the dissimilarity within the region pairs. Indeed, for each 3D plane, we can define a continuous transformation between left and right images points, stating they are the projection of a given 3D point of the reconstructed plane ; see [13, 14].

**Left-Right and Right-Left transformations, or parameterized inter-image neighbour**



We call  $T_{LR}$  the transformation which maps pixels of the left image onto the right image. The inverse transformation, from right to left, is called  $T_{RL}$ . We associate with each possible plane a transformation  $T_{LR}$  and a transformation  $T_{RL}$  (see figure 5).

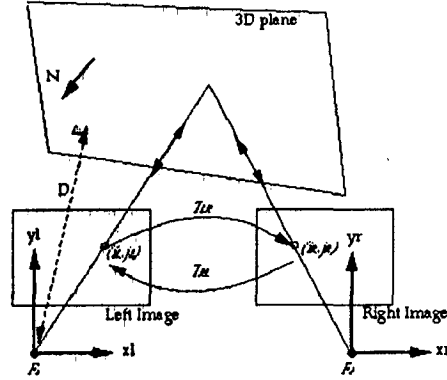


Figure 5: Transformations associated with each 3D plane

We adopt the polar representation of a 3D plane, i.e. :  $\vec{N} \cdot \vec{X} = D$ , where  $D$  is the distance of the plane to the origin of the 3D coordinate frame and  $\vec{N}$  is the unit normal to the plane. If we use the spherical representation of  $\vec{N}$ , these two transformations (continuous in image coordinates,

or sampled on pixels) are parameterized by  $\theta, \phi$  and  $D$  :

$$\vec{N} = \begin{pmatrix} \cos(\theta) \sin(\phi) \\ \sin(\theta) \sin(\phi) \\ \sin(\phi) \end{pmatrix}$$

$$(i_R, j_R) = T_{LR}(i_L, j_L, \theta, \phi, D)$$

$$(i_L, j_L) = T_{RL}(i_R, j_R, \theta, \phi, D)$$

Here  $(i_L, j_L)$  is a pixel of the left image and  $(i_R, j_R)$  of the right image. Of course, the transformation depends also on the calibration parameters of the stereo couple. We'll suppose we obtained these parameters beforehand, using calibration techniques.

With the help of this transformation between images, it is straightforward to define the terms of the coupling energy, based upon the matched regions. We propose several terms, computed on labelled or grey levels images.

#### Overlapping term

We consider that the true 3D facet must exactly project on the two matched regions. This term is thus fully efficient only in the case of non-hidden parts. For each facet, with parameters  $(\theta, \phi, D)$  and associated with two matched regions,  $A_L$  and  $A_R$  in the left and right images, the overlapping term is :

$$U_{lab} = \sum_{(i_L, j_L) \in A_L} \zeta [Lab_L(i_L, j_L) - Lab_R(T_{LR}(i_L, j_L, \theta, \phi, D))] \\ + \sum_{(i_R, j_R) \in A_R} \zeta [Lab_R(i_R, j_R) - Lab_L(T_{RL}(i_R, j_R, \theta, \phi, D))]$$

$Lab_L$  and  $Lab_R$  represent the two labelled images of the pair (matched regions have identical labels on the two images). This term is zero, the minimum value, when all the pixels of the left region are transformed by  $T_{LR}$  into pixels of the right region, and conversely using  $T_{RL}$ .  $U_{lab}$  is a measure of the overlap of the two regions.

### Grey level term

Other approaches, particularly [19], use grey level criteria. More generally, it is widely recognized that the use of color information in stereovision improves efficiency [10, 8, 11, 20, 21, 16, 12]. We thus propose a grey level term, for black and white images, or for each channel of a color image (coded in RVB, for example). For a facet, corresponding to the two regions  $A_L$  and  $A_R$ , it is written as :

$$U_{grey} = \sum_{(i_L, j_L) \in A_L} [I_L(i_L, j_L) - I_R(T_{LR}(i_L, j_L, \theta, \phi, D))]^2 + \sum_{(i_R, j_R) \in A_R} [I_R(i_R, j_R) - I_L(T_{RL}(i_R, j_R, \theta, \phi, D))]^2$$

$I_L$  and  $I_R$  are the grey level images, or one of the three channels of a color image. In this latter case the color criterion is the sum of the three grey level criteria ; we logically suppose that these criteria are equally important for each channel.

This criterion tends to match the pixels of the regions more precisely than the overlapping term, because it is minimal when the transformations  $T_{LR}$  and  $T_{RL}$  map into pixels with identical grey levels. In this way, it is more precise than the overlapping criterion. But this criterion is more fragile (especially on noisy images) than the overlapping criterion and is exact only in the case of lambertian facets. However, it is well known that in real cases this lambertian assumption is generally valid, except for strongly specular facets.

Notice also that these criteria are more discriminating when the grey levels of the regions are not uniform. In the case of uniform regions, it has the same effect as an overlapping criterion. On the other hand, this pixel to pixel matching criteria allows to handle hidden portions.

### Contour term

We have proposed label and grey levels terms, which correspond to a region-based approach to stereo matching. It is also well known that contours provide useful information. We thus propose to include a criterion based upon the image contours, whose expression for a facet is :

$$U_{contours} = \sum_{(i_L, j_L) \in A_L} \zeta [Cont_L(i_L, j_L) - Cont_R(T_{LR}(i_L, j_L, \theta, \phi, D))] + \sum_{(i_R, j_R) \in A_R} \zeta [Cont_R(i_R, j_R) - Cont_L(T_{RL}(i_R, j_R, \theta, \phi, D))]$$

$Cont_L$  and  $Cont_R$  are contour images associated with left and right images. They are computed on-line from the Label images. This criterion tends to map contour pixels of the left image onto contour pixels of the right image. Like the grey level criterion, it is more precise than the overlapping criterion, and allows us to handle hidden parts in most cases.

### Coupling energy

The coupling energy, for one pair of matched regions, is parameterized by  $\theta$ ,  $\phi$  and  $D$ , and is computed as follows :

$$U_{Coup}(\theta, \phi, D) = w_{lab} * U_{lab} + w_{grey} * U_{grey} + w_{contours} * U_{contours} \quad (1)$$

The choice of the weights is problematic. We propose weights whereby the different contributions are almost equally important ;

$$w_{lab} = w_{contours} = 1 \\ w_{grey} = \frac{1}{N} * \frac{1}{2(\sigma_L^2 + \sigma_R^2)}$$

$N$  is the number of channels (3 for color images) ;  $\sigma_L^2$  and  $\sigma_R^2$  are variances of grey levels on a left and right regions, and are parameters which must be chosen. The grey level term becomes very large when

we are sure that grey levels don't correspond to the same region; the contribution of a pair of matched pixels in the  $C_{grey}$  term stays between 0 and 1 if they could belong to the same region ; see [4] for a mathematical justification.

This function is computed by scanning the two images and is computationally expensive. In a minimization process, it must be computed for many various values of  $\theta, \phi$  and  $D$ . We proposed several criteria (see [14]) which avoid a complete computation of the function  $U_{Coupl}(\theta, \phi, D)$  for some values of  $\theta, \phi$  and  $D$ , to which we assign an arbitrarily high value to  $U_{Coupl}(\theta, \phi, D)$ .

### 3.3 Global energy

The complete energy expression is thus :

$$U(Lab_{Left}, Lab_{Right} | I_{Left}, I_{Right}) = U_{Seg}(Lab_{Left} | I_{Left}) + U_{Seg}(Lab_{Right} | I_{Right}) \\ + \alpha U_{Coupl}(Lab_{Left}, Lab_{Right} | I_{Left}, I_{Right})$$

$U_{Coupl}(Lab_{Left}, Lab_{Right} | I_{Left}, I_{Right})$  is the sum over all the pairs  $(A_L, A_R)$  of the coupling terms we have just defined. The parameter  $\alpha$  is very important because it controls the relative importance of the 2D segmentation term and the 3D coherence term.

## 4 METHODOLOGY

We wish to minimize the preceding energy expression, with respect to the labels associated with the two images of the stereo pair but also with respect to the triplet  $(\theta, \phi, D)$  of parameters defining the planes associated with each label (present in the labelled images). Moreover, we have to choose  $\alpha$ , balancing the segmentation and the coupling terms, and the other constants :  $\sigma_L^2, \sigma_R^2$  for the coupling term, and  $\sigma_{Lab}$  for the segmentation term.

In such approaches, where we have to minimize arrays and select parameters, a common solution is to use recursively a classical MRF optimization technique, followed by parameter estimation (sometimes called meta-optimization).

### 4.1 Label minimization

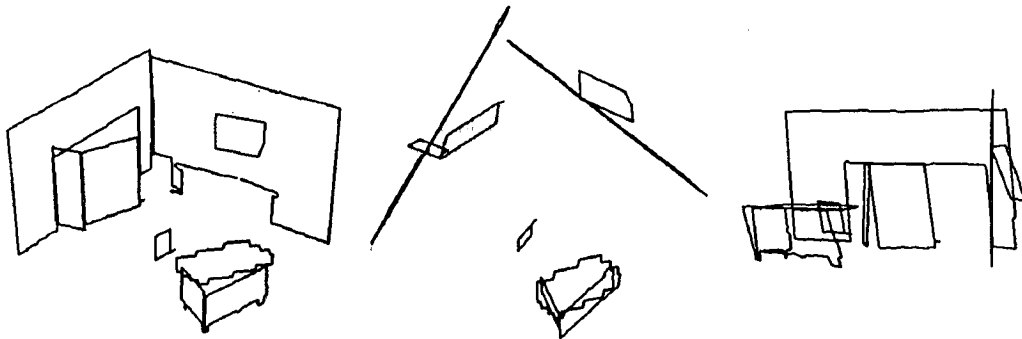
We choose the simple simulated annealing method. But considering that we have an initial guess of good quality, thus being near the global minimum, we use simulated annealing with a low initial temperature. Thus is equivalent to a low initial acceptance rate (Aragon temperature initialization method).

### 4.2 Facet minimization

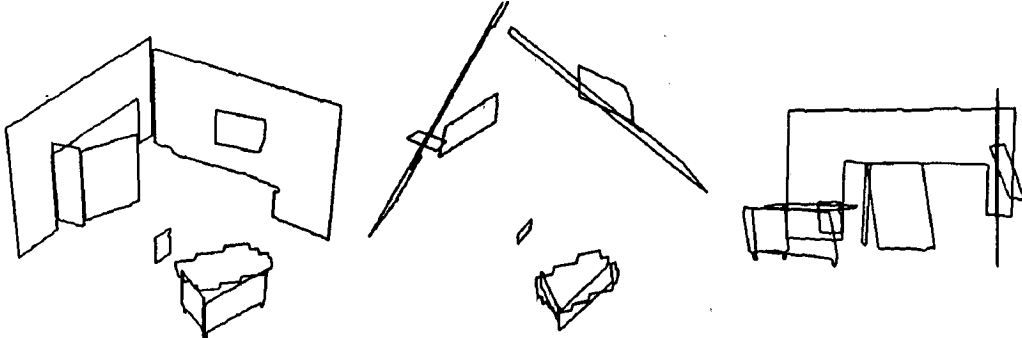
The second step of the minimization process is the minimization of the coupling term with respect to the parameters of the planes. In order to reduce the computing time we do a separate minimization for each facet. Indeed, the minimization of the coupling term is separable with respect to the triplets  $(\theta, \phi, D)$  associated with each match of the stereo pair. And, in that case, we do not need to scan the whole image to compute the coupling term associated with each match. Scanning the circumscribing rectangle of the regions is sufficient. Thus, for each match of the stereo pair, we search for an associated plane, which is the supporting plane of the reconstructed 3D facet. Left and right regions on the images are projections of this facet.

The principal problem of minimizing such functions is to avoid local minima ; indeed it is evident that the preceding functionals have irregular forms, especially in their sampled versions. In order to reduce the computation time, we progressively compute the minimum with the help of approximations of the reconstruction function, using a coarse-to-fine approach ; see [13, 14]. These functions are computed on a larger grid, i.e., we make  $N$  divisions in  $x$  and  $y$  of the circumscribing rectangle of the regions, and compute the reconstruction function using the nodes of this new grid as "big" pixels. The minimum of these functions are near the minimum of the full-scale reconstruction function, but their computation is quicker. We use simple gradient descent to minimize these functions, using the minimum of one function as initial estimation for the higher scale function, until we reach full scale resolution.

## 5 RESULTS



First reconstruction, only with coupling energy : perspective view - upper view - right view



Final reconstruction, with both energies : perspective view - upper view - right view

Figure 6: Reconstruction results on the simulated data

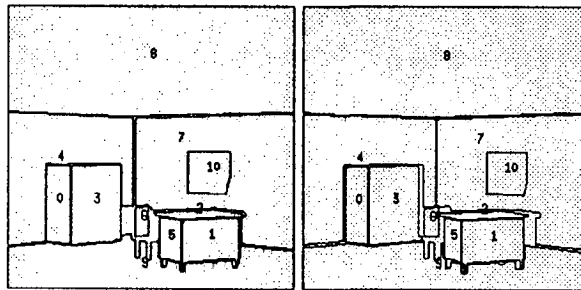


Figure 7: Segmentation and matching results on the simulated data. Final segmentation and matching, after minimization process.

We first tested our algorithms on synthetic data. We present comparative results, with the “static” method, of minimization of only the coupling term, described in [13, 14]. Figure 6 shows the reconstruction results of this method on a synthesized office scene (generated with the INRIA-SOGITEC modeler [2]). Figure 7 shows the modification on the segmented and matched pair due to the minimization process. Of course, in some pathological cases the reconstruction is impossible (for the ceiling of the synthesized pair, for example), due to lack of information. In this case the modification between static and MRF methods

is small, due to the initial good results (knowing the theoretical precision limits, see [13, 14]). Notice the modified position of the window on the right wall ; the form and orientations of the two walls are also slightly modified. The influence of MRF technique is noticeable on the figure 7, where the unmatched regions are unclassified. (There are regions with no number on the figure 7 ; see for example the wall below the chair and the desk.)

Figures 8 to 10 show the results of our reconstruction algorithm on a real color stereo pair, taken with a CCD camera. On figure 9 we can remark the lightning effects on the top left of facet 19, this is due to the uniformity criterion based on intensity measures (photometric considerations would surely improve these segmentations). We show in figure 10 only the facets corresponding to the three biggest matched regions. In the final reconstruction, the facet 19 is correctly positionned (almost perpendicular to the floor), while the facet 10 (right wall) remains trapped in a local minimum (this is due to the minimization process, see [14])

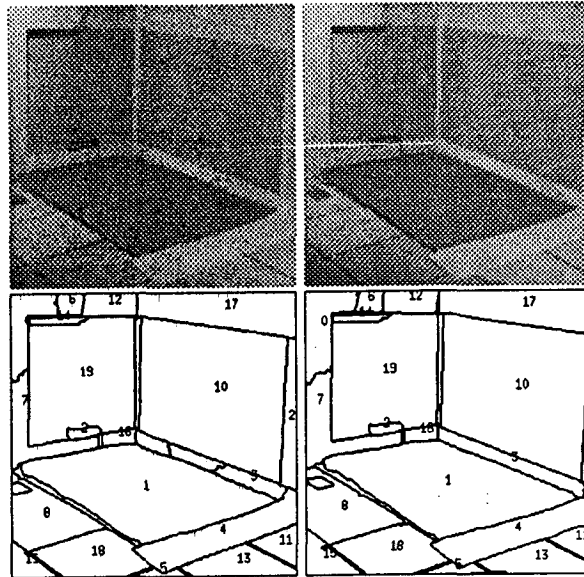


Figure 8: Real color stereo pair, red channel, and matching

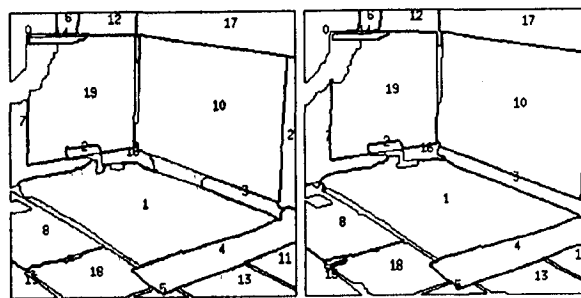
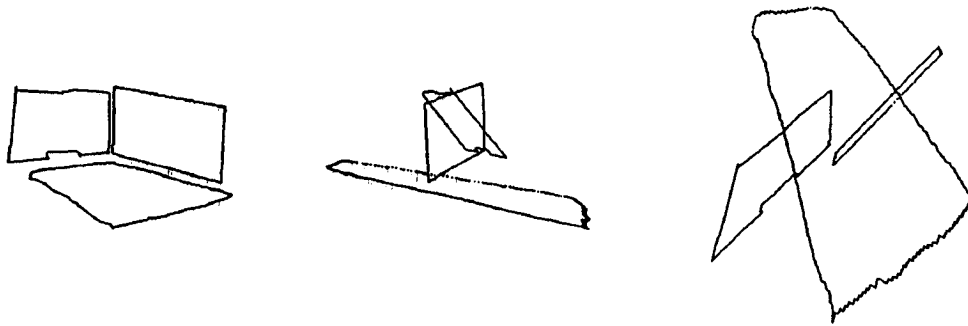
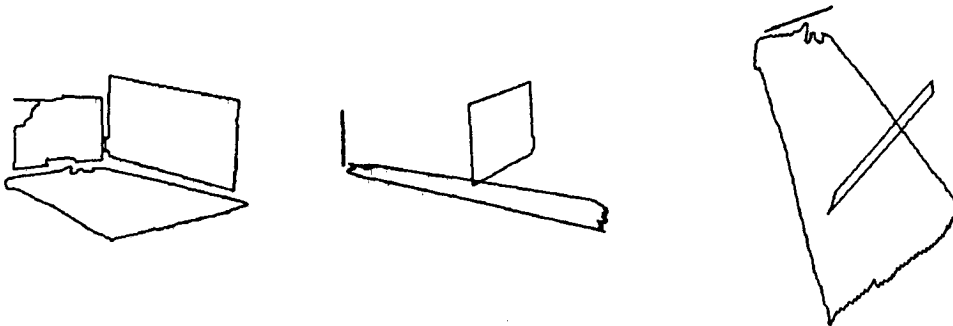


Figure 9: Final matching, produced after minimization



First reconstruction, only with coupling energy : front view - left view - upper view



Final reconstruction, with both energies : front view - left view - upper view

Figure 10: Results on the real scene

## 6 CONCLUSION AND PERSPECTIVES

We have proposed a reconstruction method, which allows refinement of the a priori segmentation and matching, with help of a Markov Random Field approach. This iterative or feedback step improves reconstruction results, in comparison with the "static" 3D reconstruction method presented in [13] and in [14].

The method that we have presented is easily extendable, particularly the energy expressions. We can improve the efficiency of the segmentation process by adding a line process in the image energies, and we can also improve the coupling energy by including some photometrical considerations (see [14]), and by considering other surface primitives (with obvious modifications of left-right and right-left transformations expressions).

We intend to extend the presented method in three ways :

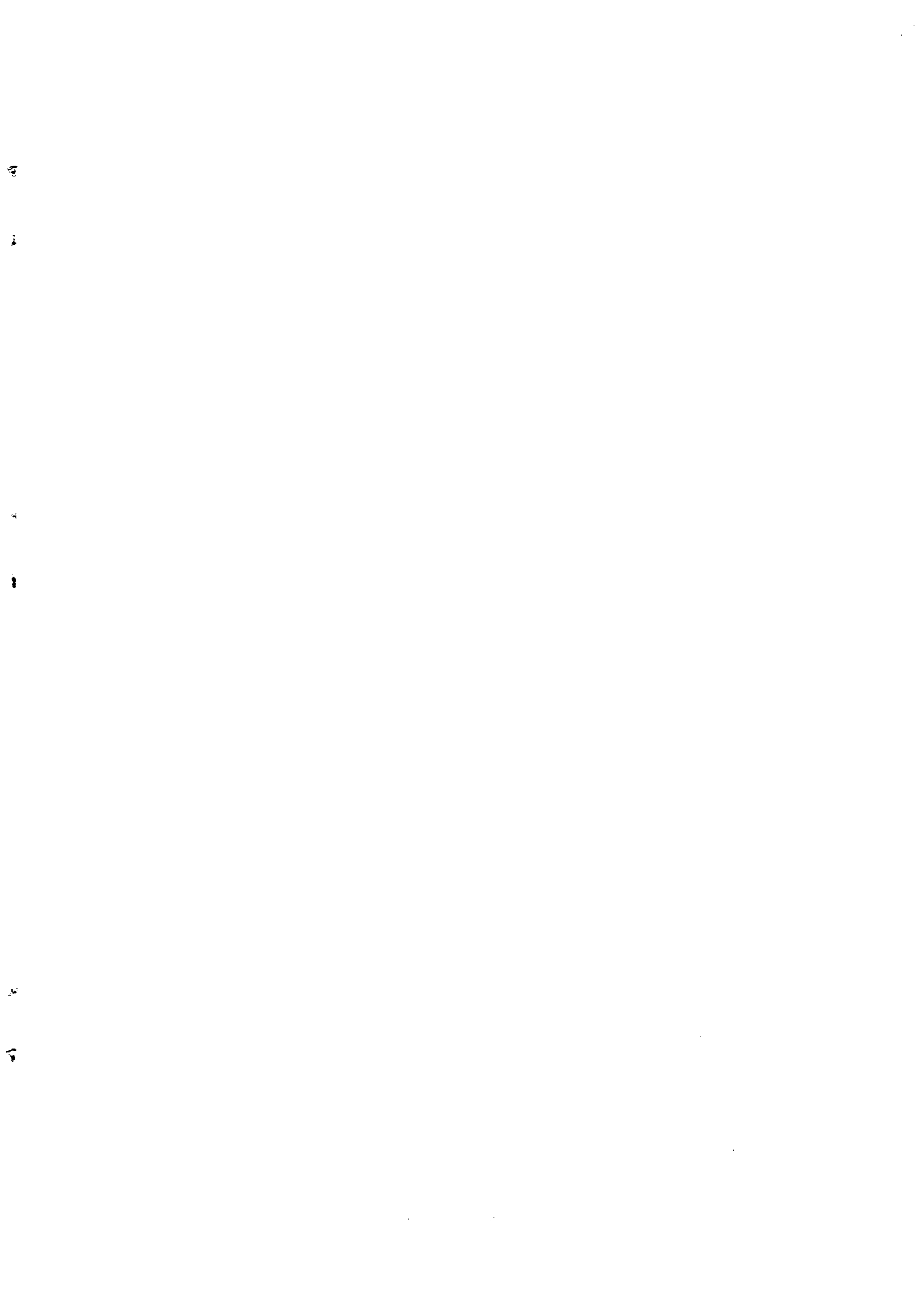
- to create a complete stereo reconstruction algorithm which does not require as an initial guess an a priori segmentation and matching (we are currently studying multiscale approaches),
- to study various extensions, especially including the photometric considerations, in order to handle specular surfaces,
- to study parallel implementations to ameliorate the computational difficulties.

## 7 ACKNOWLEDGMENTS

I would like to thank Donald GEMAN for his encouragement, and for the corrections made to this manuscript.

## References

- [1] G. L. Bilbro and W. E. Snyder. Fusion of range and image data using markov random fields. In *IEEE International Symposium on Intelligent Control*, pages 154-158, 1988. 24-26 August, Arlington, Virginia.
- [2] P. J. Brock, S. Coquillart, and F. Cros. Conception et implémentation d'un modèleur géométrique interactif. *Bigre*, 61-62:139-144, April 1989. Langages et algorithmiques du graphique.
- [3] J. M. Bruneau, M. Barlaud, and L. Blanc-Féraud. Stereo surface reconstruction using markov random fields and wavelets' pyramids. Rapport de Recherche 92-14, I3S, CNRS URA 1376, Université de Nice - Sophia Antipolis, February 1992.
- [4] B. Cernuschi-Frias, D. B. Cooper, Y. P. Hung, and P. N. Belhumeur. Towards a model-based bayesian theory for estimating and recognizing parameterized 3d objects using two or more images taken from different positions. *IEEE Trans. on Pattern Analysis and Machine Intelligence*, 11(10):1028-1052, October 1989.
- [5] S. Chatterjee and C. Chang. Stochastic approaches to early vision : Stereo disparity. In *24th Asilomar Conference on Signals, Systems and Computers*, pages 539-544, 1990. November 5-7, California.
- [6] D. Geman. Stochastic model for boundary detection. *Image and Vision Computing*, 5(2):61-65, May 1987.
- [7] S. Geman and D. Geman. Stochastic relaxation, gibbs distributions, and the bayesian restoration of images. *IEEE Trans. on Pattern Analysis and Machine Intelligence*, 6(6):712-741, November 1984.
- [8] G. Healey and T. O. Binford. The role and use of color in a general computer vision system. In *Image Understanding Workshop (DARPA)*, pages 599-613, February 1987. Los Angeles.
- [9] F. Heitz, E. Memin, and P. Bouthemy. Markov random fields and parallel algorithms for 2d motion analysis. In *13th Imacs World Congress on Computation and Applied Mathematics*, 1991. Dublin, July.
- [10] J. R. Jordan and A. C. Bovik. Computational stereo vision using color. *IEEE Control Systems Magazine*, pages 31-36, June 1988.
- [11] R. S. Ledley, M. Buas, and T. J. Golab. Fundamentals of true color image processing. In *10th Int. Conference on Pattern Recognition*, pages 791-796, 1990. Atlantic City, New Jersey, USA, 16-21 June.
- [12] Q. T. Luong. La couleur en vision par ordinateur : 1 - une revue. Technical Report 1251, INRIA, Juin 1990.
- [13] E. Lutton, J.-M. Vezien, and A. Gagalowicz. About criteria for 3d reconstruction of planar facets from a stereo pair. In *ISCIS VII*, 1992. 2-4 November, Antalya, Turkey.
- [14] E. Lutton, J.-M. Vezien, and A. Gagalowicz. Model-based stereo reconstruction by energy minimization. In *IMAGE'COM 93*, 1993. 23-25 Mars, Bordeaux, France.
- [15] J. L. Marroquin. A probabilistic approach to computational vision. *Image Understanding*, pages 44-80, 1989. Editor : S. Ullman, W. Richards.
- [16] A. Pentland. Photometric motion. In *Proceedings ICCV*, pages 178-187, 1990.
- [17] Y. Remion. *Stéréovision par zones, outils et structures d'un système expert*. PhD thesis, Télécom Paris, Juin 1988. 88E015.
- [18] P. T. Sander, L. Vinet, L. Cohen, and A. Gagalowicz. Hierarchical regions based stereo matching. In *Proceedings of the Sixth Scandinavian Conference on Image Analysis*, pages 71-78, Oulu, Finland, June 1989.
- [19] J. Subrahmonia, Y. P. Hung, and D. B. Cooper. Model-based segmentation and estimation of 3d surfaces from two or more intensity images using random markov fields. In *10th International Conference on Pattern Recognition*, pages 390-398, 1990. Atlantic City, New Jersey, USA, 16-21 June.
- [20] H. D. Tagare and R. J. P. DeFigueiredo. Simultaneous estimation of shape and reflectance maps from photometric stereo. In *Third International Conference in Computer Vision*, pages 340-343, 1990. Dec 4-7, Osaka, Japan.
- [21] M. Tsukada and Y. Ohta. An approach to color constancy using multiple images. In *Third International Conference in Computer Vision*, pages 385-289, 1990. Dec 4-7, Osaka, Japan.
- [22] J.M. Vezien and A. Gagalowicz. Reconstruction 3-D basée sur une analyse en régions d'une paire d'images stéréoscopiques. In *Congrès AFCEP-RFIA*, 1991. Lyon - Villeurbanne, France, 25-29 Novembre.
- [23] L. Vinet, P. T. Sander, L. Cohen, and A. Gagalowicz. Cooperative segmentation and stereo matching. In *Topical Meeting on Image Understanding and Machine Vision*, North Falmouth, Massachusetts, June 1989.
- [24] W. Luo and H. Maitre. Using surface model to correct and fit disparity data in stereo vision. In *10th ICPR*, pages 60-64, 1990. Atlantic City 16-21 June.







---

**Unité de Recherche INRIA Rocquencourt**  
**Domaine de Voluceau - Rocquencourt - B.P. 105 - 78153 LE CHESNAY Cedex (France)**  
Unité de Recherche INRIA Lorraine Technopôle de Nancy-Brabois - Campus Scientifique  
615, rue du Jardin Botanique - B.P. 101 - 54602 VILLERS LES NANCY Cedex (France)  
Unité de Recherche INRIA Rennes IRISA, Campus Universitaire de Beaulieu 35042 RENNES Cedex (France)  
Unité de Recherche INRIA Rhône-Alpes 46, avenue Félix Viallet - 38031 GRENOBLE Cedex (France)  
Unité de Recherche INRIA Sophia Antipolis 2004, route des Lucioles - B.P. 93 - 06902 SOPHIA ANTIPOLIS Cedex (France)

---

**EDITEUR**  
**INRIA - Domaine de Voluceau - Rocquencourt - B.P. 105 - 78153 LE CHESNAY Cedex (France)**

ISSN 0249 - 6399

